ELSEVIER

Journal of Nuclear Materials 307–311 (2002) 283–288

journal of nuclear materials

www.elsevier.com/locate/jnucmat

Phase stability of oxide dispersion-strengthened ferritic steels in neutron irradiation

S. Yamashita [a,*], K. Oka [a], S. Ohnuki [a], N. Akasaka [b], S. Ukai [b]

[a] *Laboratory of Advanced Materials, Materials Science Division, Graduate School of Engineering, Hokkaido University N-13, W-8, Sapporo 060-8628, Japan*

[b] *Oarai Engineering Center, Japan Nuclear Cycle Development Institute, 4002 Narita-cho, Oarai-machi, Ibaraki 311-1393, Japan*

Abstract

Oxide dispersion-strengthened ferritic steels were irradiated by neutrons up to 21 dpa and studied by microstructural observation and microchemical analysis. The original high dislocation density did not change after neutron irradiation, indicating that the dispersed oxide particles have high stability under neutron irradiation. However, there is potential for recoil resolution of the oxide particles due to ballistic ejection at high dose. From the microchemical analysis, it was implied that some of the complex oxides have a double-layer structure, such that TiO_2 occupied the core region and Y_2O_3 the outer layer. Such a structure may be more stable than the simple mono-oxides. Under high-temperature irradiation, Laves phase was the predominant precipitate occurring at grain boundaries α phase and χ phase were not observed in this study.

1. Introduction

Oxide dispersion-strengthened (ODS) ferritic steels have excellent high-temperature mechanical properties attributed to the oxide dispersion and high swelling resistance, which is an inherent characteristic of ferritic steels. Because of these properties, ferritic steels are considered to be prospective candidate materials for long-life fuel cladding tubes of fast breeder reactors and, at present, are planned to vie for first wall components of fusion reactors with other high-temperature materials.

Primary issues in developing ODS ferritic steels for nuclear applications materials are whether the formability can be improved and whether severe ductility loss can be prevented or reduced; both properties are indispensable in a tube fabrication process. These problems have been successfully overcome by controlling the microstructure using techniques such as a recrystallization heat-treatment [1–4] and gamma-to-martensite phase transformation [5]. Simultaneously, these microstructural controlling techniques also contribute to the reduction of anisotropy in creep rupture strength [4,5]. From recent studies on alloying design and fabrication processes, it has been shown that advanced ODS ferritic steels before neutron irradiation have superior mechanical properties with fine, uniformly distributed oxide particles in their microstructures [6]. There is, however, only limited data on neutron-irradiated ODS ferritic steel, because most of these steels are still under irradiation in experimental reactors. Therefore, understanding microstructural behavior during neutron irradiation in ODS ferritic steels is far from sufficient. For example, how long would oxide particles be stable under neutron irradiation? Would there be unexpected secondary phase formation? Would dislocation densities increase or decrease?

In this work, we investigated the phase stability of neutron-irradiated ODS ferritic steels [7], which had been previously designed and manufactured in thin-walled tubes having similar composition to the advanced ODS ferritic steels [6].

* Corresponding author. Tel.: +81-11 706 6771; fax: +81-11 706 6772.

E-mail address: yamashita.shinichirou@jnc.go.jp (S. Yamashita).

0022-3115/02/$ - see front matter
PII: S0022-3115(02)01077-2

2. Experimental procedure

2.1. Materials

The materials are Fe–0.09C–10.98Cr–2.67W–0.4Ti–0.63Y_2O_3 (hereafter designated as 1DS) and Fe–0.046C–12.76Cr–2.81W–0.57Ti–0.34Y_2O_3 (hereafter designated as 1DK). The number correspond to element concentration in mass%. Details of the chemical composition and the tube manufacturing process have been published [7].

2.2. Irradiation condition and microstructural observation

Fast neutron irradiation was performed at a temperature between 723 and 834 K to a fluence of 2.1–4.2×10^{26} n/m^2 ($E > 0.1$ MeV), which is equivalent to 10.5–21.0 dpa, respectively, in the experimental fast reactor JOYO.

Specimens were sliced from the cladding tube and were mechanically thinned to 0.2 mm, from which 3 mm discs were punched. These discs were electro-polished with an electrolytic solution of $CH_3COOH:HClO_4 = 19:1$.

All of the microstructural observations were performed on a JEOL 4000FX electron microscope with STEM/EDS operated at 400 kV.

3. Results

3.1. Microstructure

Microstructures of 1DK and 1DS before irradiation are shown in Fig. 1(a) and (b), respectively. Grains were extremely elongated parallel to the extrusion direction during tube manufacturing. After irradiation, no significant structural changes were observed at low magnification, as seen in Fig. 1(c) and (d). The dislocation densities of 1DK and 1DS after irradiation were measured from typical micrographs and are shown in Fig. 2 as a function of temperature. The dislocation density of each steel before irradiation was 3.19×10^{14} and

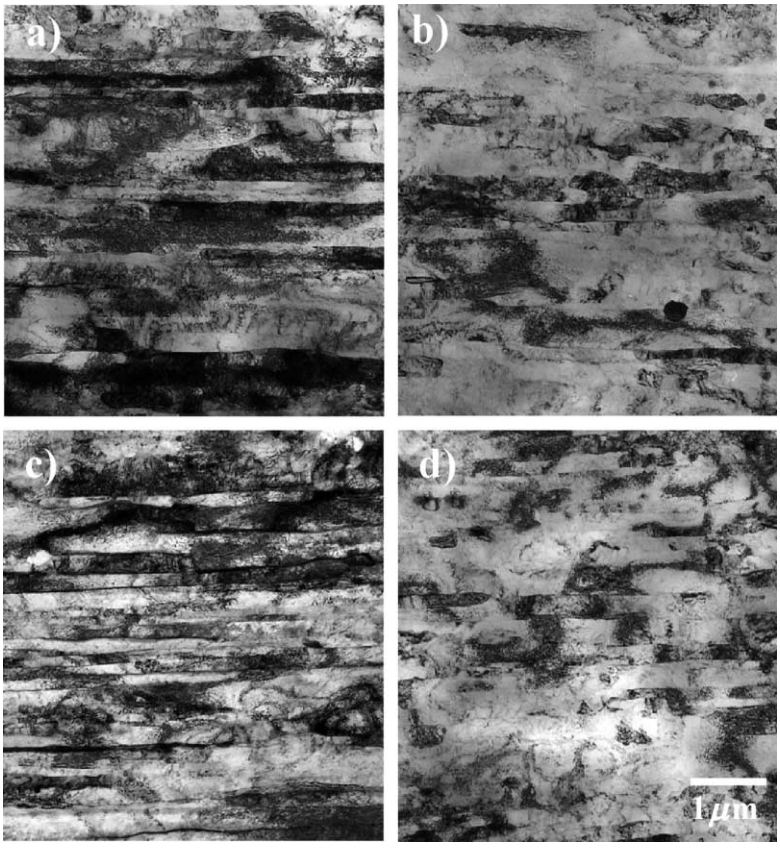

Fig. 1. Microstructures of 1DK (a) before and (c) after irradiation at 834 K to 10.5 dpa, and those of 1DS (b) before and (d) after irradiation at 723 K to 18.0 dpa.

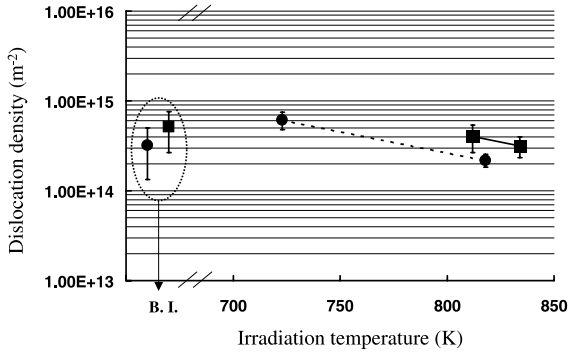

Fig. 2. Temperature dependence of dislocation density in 1DK (solid square) and 1DS (solid circle). The dislocation density of each steel before irradiation is also plotted by the same symbols within dashed circle.

5.13×10^{14} m^{-2}, for 1DS and 1DK, respectively, and these are shown in Fig. 2 for reference. Dislocation density decreased slightly with an increase in temperature, but remained high at around 10^{14} m^{-2} even after irradiation. Furthermore, no detectable void formation was observed in the high magnification images, which indicated both ODS ferritic steels had a high swelling resistance at these irradiation conditions.

3.2. Stability of oxide particles

Fig. 3 shows dark-field images of dispersed oxide particles in both ODS steels before and after neutron irradiation. Before irradiation, the distribution of the oxide particles in 1DS was finer than in 1DK. However, after irradiation, most of fine particles (less than a few nm) disappeared and those of average size in both steels seemed to grow slightly with increasing irradiation dose or temperature. To get detailed information on the stability of oxide particles during irradiation, the number density and mean size of the oxide particles were measured with micrographs, and these are plotted in Fig. 4(a) as a function of temperature for 1DS and (b) as a function of dose for 1DK. In Fig. 4(a), although both number density and mean particle size decreased with neutron irradiation, the oxide distribution remained nearly constant both in the average size and number density even with increasing temperature. On the other hand, in Fig. 4(b), the mean particle size grew slightly, whereas both the particle number density and the width of the scatter band decreased with increasing dose. These results indicated that recoil resolution of fine oxide particles might take place due to neutron irradiation and that the stability of oxide particles was more sensitive to dose than temperature.

3.3. Identification and configuration of oxide particles

The STEM/EDS microchemical analysis results of oxide particles for pre- and post-irradiation steels are summarized in Table 1. There were two types of oxide particles; one was a TiO_2 type containing over 98 wt% titanium, and the other was a complex Ti + Y oxide type containing more than 47 wt% yttrium. From the X-ray

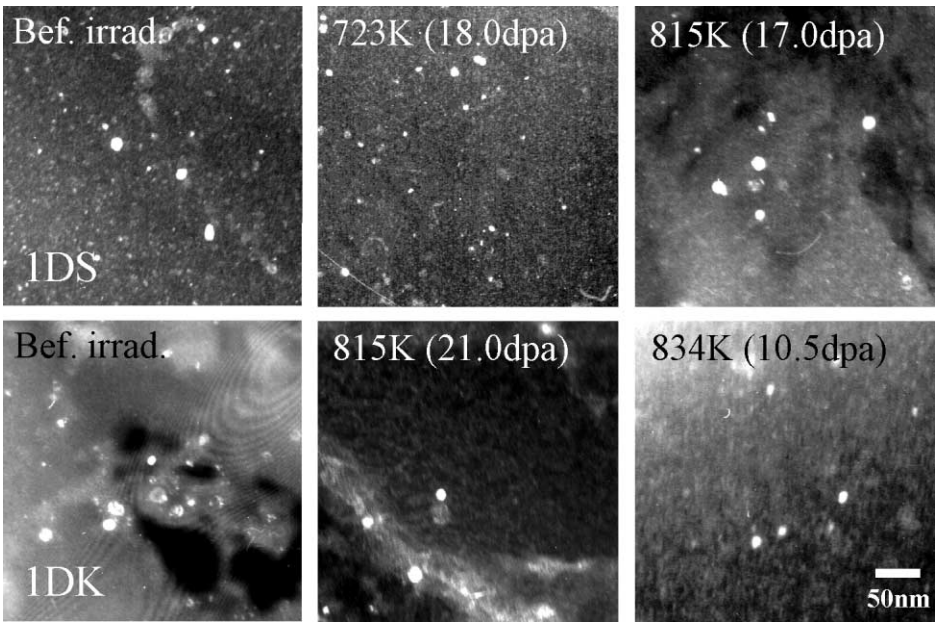

Fig. 3. Dark-field images of oxide particles in 1DS (upper side) and 1DK (lower side) before and after neutron irradiation.

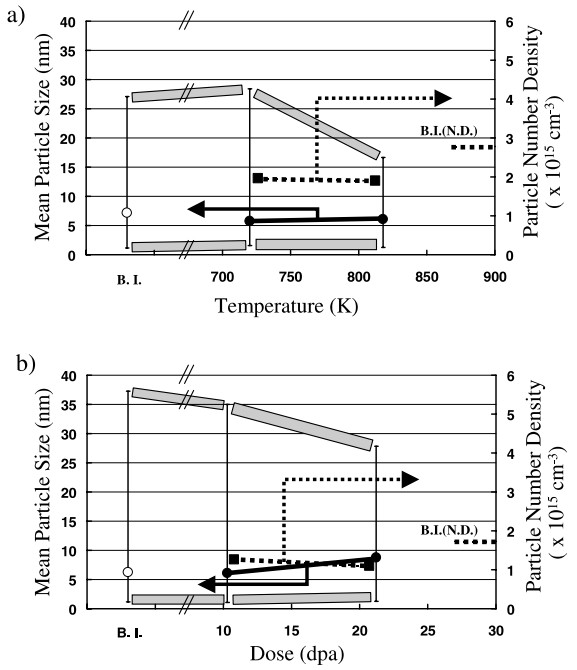

Fig. 4. (a) Temperature dependence in 1DS at the same dose level (17.0, 18.0 dpa), and (b) dose dependence in 1DK at the same temperature range (815, 834 K) of mean particle size (left *Y*-axis) and particle number density (right *Y*-axis).

diffraction analysis of Okuda et al. [8] in annealed ODS powder, there is the possibility of the presence of Y_2TiO_5 and $Y_2Ti_2O_7$, but it was not possible to accurately determine this.

A peculiar feature on the configuration of oxides before and after irradiation was found through the microchemical analysis and is shown in Table 2. Relatively large titanium oxide (>60 nm) particles showed different compositions at the center and at the edge. At the center, the metallic element was mostly Ti, and little Y was detected. At the edge, the Ti concentration decreased, and Y increased by more than a factor of 2.

Table 1
Composition of metallic elements of oxide particles in 1DK before and after irradiation (mass%)

	Ti	Yi	Y/T
TiO_2 type			
Unirradiated	98.99	1.01	0.010
10.5 dpa (834 K)	99.06	0.94	0.010
21.0 dpa (815 K)	98.12	1.88	0.019
Y + Ti complex oxide type			
Unirradiated	32.33	67.67	2.093
10.5 dpa (834 K)	34.83	65.17	1.871
21.0 dpa (815 K)	52.45	47.55	0.906

Table 2
Composition of metallic elements measured by STEM/EDS of TiO_2 type particles in 1DK before and after irradiation (mass%)

	Ti	Y	Y/Ti
a (Unirradiated)	97.19	2.81	0.029
	(95.27)	(4.73)	(0.050)
b (Unirradiated)	99.86	0.14	0.001
	(98.93)	(1.07)	(0.011)
c (21.0 dpa, 815 K)	97.53	2.47	0.025
	(97.14)	(2.86)	(0.029)
d (21.0 dpa, 815 K)	99.78	0.22	0.002
	(98.46)	(1.54)	(0.016)

Values in brackets are local composition at the edge part of the particle.

3.4. Precipitation

Precipitates with rod-like structure were formed at most grain boundaries in both steels at irradiation temperatures between 815 and 834 K, whereas no precipitate formation occurred at 723 K. Typical bright and dark-field images of 1DS are shown in Fig. 5. Precipitates only formed at the grain boundaries. The chemical analysis revealed that the precipitate was comprised of the metallic elements Fe, Cr and W. From the results of chemical and diffraction pattern analyses, these precipitates were identified as W-based Laves phase. Other important precipitate formation, such as phase or χ phase, were not observed.

4. Discussion

4.1. Microstructure

The dislocation density remained high even after irradiation. It is proposed that the reason was because the dispersed oxide particles pinned and interfered with the movement of dislocations during irradiation. Microstructural evaluation revealed no detectable voids at dose levels up to 21 dpa. In the case of the ODS steels examined, the number density of annihilation sites of defect clusters produced by neutron irradiation, such as dislocations and oxide particle interfaces [9], would be very high compared with non-ODS steels, and they would contribute to the suppression of the concentration of defect clusters in the matrix during irradiation.

4.2. Oxide particle stability under irradiation

Both Y_2O_3 and the complex Ti + Y oxides are considered to be thermodynamically stable at elevated temperature, even above 2273 K [8,10], and they are also reported to be very stable under irradiation by ions [11,12], electrons [9,13,14] and neutrons [15]. It was,

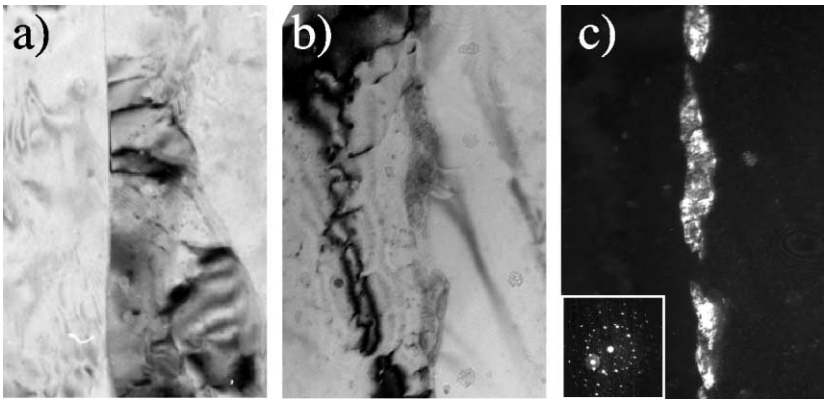

Fig. 5. Grain boundary structures of 1DS irradiated at (a) 723 K and (b) 815 K. (c) Dark-field contrast of Laves phase corresponding to (b).

Table 3
Volume fraction of oxide particles measured from micrographs before and after irradiation (%)

	1DK	1DS
Unirradiated	0.13	0.18
723 K	–	0.09 (18.0 dpa)
815 K	0.13 (21.0 dpa)	0.06 (17.0 dpa)
834 K	0.07 (10.5 dpa)	–

however, suspected by Dubuisson et al. [16] that those oxide particles having high-temperature stability might not be so stable at high doses (>75 dpa) of neutron irradiation due to recoil resolution of oxide particles attributed to the ballistic ejection of oxide atoms by impinging neutrons. Taking into account both the scattering width reduction in particle size with increasing dose (Fig. 4(b)) and the decrease in volume fraction after irradiation (Table 3), the results of the present work imply that there is the possibility of oxide particle dissolution induced by neutron irradiation.

4.3. Precipitate formation under irradiation

Under high-temperature irradiation (815 and 834 K), W-based Laves phase formed on grain boundaries in both steels. The predominant factor dictating Laves phase formation is thermal rather than irradiation effects, since Laves phase generally precipitates during thermal aging at high temperature [17,18].

5. Conclusion

To investigate the phase stability in the previously developed ODS ferritic steels after neutron irradiation, microstructural observations and chemical analyses were performed. The results can be summarized as follows:

(1) Two types of ODS ferritic steels examined in this study had a high swelling resistance because the high density of dislocations and oxide particles can act as effective sinks for point defects.
(2) Oxide particles were relatively stable up to ~21 dpa, but the average size increased slightly at higher doses, which implies the possibility of recoil resolution of the oxide particles during neutron irradiation.
(3) Some of large oxides had different compositions at the center and at the edge. This configuration of oxides may be more stable thermodynamically than simple a mono-oxide, such as Y_2O_3 and TiO_2.
(4) W-based Laves phase formed after neutron irradiation at 815 and 834 K.

References

[1] S. Ukai, M. Harada, H. Okada, M. Inoue, S. Nomura, S. Shikakura, K. Asabe, T. Nishida, M. Fujiwara, J. Nucl. Mater. 204 (1993) 65.
[2] S. Ukai, M. Harada, H. Okada, M. Inoue, S. Nomura, S. Shikakura, T. Nishida, M. Fujiwara, K. Asabe, J. Nucl. Mater. 204 (1993) 74.
[3] H. Okada, S. Ukai, M. Inoue, J. Nucl. Sci. Technol. 33 (12) (1996) 936.
[4] S. Ukai, T. Nishida, H. Okada, J. Nucl. Sci. Technol. 34 (3) (1997) 256.
[5] S. Ukai, T. Nishida, H. Okada, T. Yoshitake, J. Nucl. Sci. Technol. 35 (4) (1998) 294.
[6] S. Ukai, JNC Tech. Rev. 7 (2000) 83 (in Japanese).
[7] T. Yoshitake, T. Ohmori, S. Miyakawa, J. Nucl. Mater. (paper for ICFRM-10), in preparation.
[8] T. Okuda, M. Fujiwara, J. Mater. Sci. Lett. 14 (1995) 1600.
[9] S. Yamashita, S. Watanabe, S. Ohnuki, H. Takahashi, N. Akasaka, S. Ukai, J. Nucl. Mater. 283–287 (2000) 647.
[10] R.S. Roth, A.E. Mchale, J. Am. Ceram. Soc. 69 (1986) 827.
[11] E.A. Little, D.S. Mazey, W. Hanks, Scripta Metall. Mater. 25 (1991) 1115.

[12] K. Asano, Y. Kohno, A. Kohyama, T. Suzuki, H. Kusanagi, J. Nucl. Mater. 155–157 (1988) 928.
[13] H. Kinoshita, N. Akasaka, H. Takahashi, I. Shibahara, S. Onose, J. Nucl. Mater. 191–194 (1992).
[14] J. Saito, T. Suda, S. Yamashita, S. Ohnuki, H. Takahashi, N. Akasaka, M. Nishida, S. Ukai, J. Nucl. Mater. 258–263 (1998) 1264.
[15] D.S. Gelles, Report DOE/ER-0313/16, 1994, p. 146.
[16] P. Dubuisson, R. Schill, M. Hugon, I. Grislin, J. Seran, ASTM STP 1325 (1999) 882.
[17] Y. Kohno, D.S. Gelles, A. Kohyama, M. Tamura, A. Hishinuma, J. Nucl. Mater. 191–194 (1992) 968.
[18] M. Tamura, H. Hayakawa, A. Yoshitake, A. Hishinuma, T. Kondo, J. Nucl. Mater. 155–157 (1988) 620.